The Influence of Interplanetary Magnetic Field Direction on Martian Crustal Magnetic Field Topology

Tristan Weber, David Brain, Shaosui Xu, David Mitchell, Jared Espley, Jasper Halekas, Christian Mazelle, Robert Lillis, Gina Dibraccio, Bruce Jakosky

AGU ADVANCING EARTH AND SPACE SCIENCE

Geophysical Research Letters

RESEARCH LETTER

10.1029/2020GL087757

The Influence of Interplanetary Magnetic Field Direction on Martian Crustal Magnetic Field Topology

Tristan Weber[1], David Brain[1], Shaosui Xu[2], David Mitchell[2], Jared Espley[3], Jasper Halekas[4], Christian Mazelle[5], Robert Lillis[2], Gina DiBraccio[3], and Bruce Jakosky[1]

[1]Laboratory for Atmospheric and Space Physics, University of Colorado Boulder, Boulder, CO, USA, [2]Space Science Laboratory, University of California, Berkeley, CA, USA, [3]Goddard Space Flight Center, Greenbelt, MD, USA, [4]Department of Physics and Astronomy, University of Iowa, Iowa City, IA, USA, [5]IRAP, CNRS-University of Toulouse-UPS-CNES, Toulouse, France

Key Points:

- Interplanetary magnetic field direction determines which crustal magnetic field cusps are open or closed to the solar wind
- Crustal fields frequently transition between closed and open topology as they rotate through the nightside of Mars
- As cusp fields reconnect with open field lines in the magnetotail, they form large closed field lines linking the dayside and nightside of Mars

Correspondence to:
T. Weber,
tristan.weber@colorado.edu

Citation:
Weber, T., Brain, D., Xu, S., Mitchell, D., Espley, J., Halekas, J., et al. (2020). The influence of interplanetary magnetic field direction on Martian crustal magnetic field topology. *Geophysical Research Letters*, *47*, e2020GL087757. https://doi.org/10.1029/2020GL087757

Received 1 MAR 2020
Accepted 24 AUG 2020
Accepted article online 30 AUG 2020

Abstract Crustal magnetic fields influence a range of plasma processes at Mars, guiding the flow of energy from the solar wind into the planet's atmosphere at some locations while shielding the atmosphere at others. In this study we investigate how the topology of crustal fields varies with changes in the direction of the incoming interplanetary magnetic field (IMF). Using plasma measurements from Mars Atmosphere and Volatile Evolution (MAVEN) and Mars Global Surveyor (MGS), we identify magnetic topology throughout the Martian ionosphere and perform a statistical analysis of crustal magnetic field topology during different IMF configurations. We find that the topology of crustal field cusp regions is dependent on IMF direction and that cusps transition between open and closed topology regularly as they rotate through the nightside of Mars. Finally, we determine that cusps often become topologically closed due to reconnection with open magnetic fields in the Martian magnetotail, creating large closed loops that connect the dayside and nightside of Mars.

1. Introduction

The flow of charged particles in and out of the Martian ionosphere is in many areas controlled by the presence of crustal magnetic fields (Acuna et al., 1998), regions of remanent magnetization that are scattered nonuniformly across the planet's surface (see Figure 1a). As these crustal fields interact and reconnect with the interplanetary magnetic field (IMF), they create a complex and dynamic magnetic system that controls both solar wind energy input and low-energy ion outflow from the planet. Energetic electrons from the solar wind precipitate along these magnetic fields, depositing their energy into the planet's atmosphere (Dubinin, Fraenz, Woch, Roussos, et al., 2008; Lillis et al., 2009, 2018; Lillis & Brain, 2013; Xu et al., 2014). This deposition is second only to solar photon absorption as an atmospheric energy source (Fox et al., 1993), and leads to local heating (Fox & Dalgarno, 1979; Krymskii et al., 2004; Sakai et al., 2016), impact ionization (Fillingim et al., 2007, 2010; Lillis et al., 2011; Lillis & Fang, 2015; Němec et al., 2011), and the production of aurora (Brain, Halekas, et al., 2006; Haider et al., 1992; Leblanc et al., 2008). Magnetic fields also constrain the movement of escaping low-energy ions, regulating the ion outflow processes that may have contributed to substantial atmospheric loss over time (Collinson et al., 2015; Ergun et al., 2016; Harnett & Winglee, 2006; Jakosky et al., 2018; Ma et al., 2014; Nilsson et al., 2011; Ramstad et al., 2016).

It is therefore useful for us to evaluate where and when magnetic fields allow for direct connection between the solar wind and the ionosphere, an area of study referred to as magnetic topology. In analyzing topology we differentiate between cases when magnetic field lines are (1) connected only to Mars (closed), (2) connected only to the solar wind (draped), or (3) connected to both Mars and the solar wind (open). These distinctions inform us of which locations at Mars are exposed to solar wind energy input and reveal where and how ion outflow is likely to occur. As such, magnetic topology has been the subject of a several different studies at Mars, including statistical analyses of magnetic topology across the planet (Brain et al., 2007; Luhmann et al., 2015; Weber et al., 2017; Xu et al., 2017, 2019), as well as many studies that used topological analysis as a baseline for understanding unique phenomena in the Martian space environment (e.g., Brain et al., 2010; Dubinin, Fraenz, Woch, Winnigham, et al., 2008; Eastwood et al., 2008; Frahm et al., 2006; Leblanc et al., 2006; Liemohn, Ma, Frahm, et al., 2007; Liemohn, Ma, Nagy, et al., 2007; Mitchell et al., 2001).

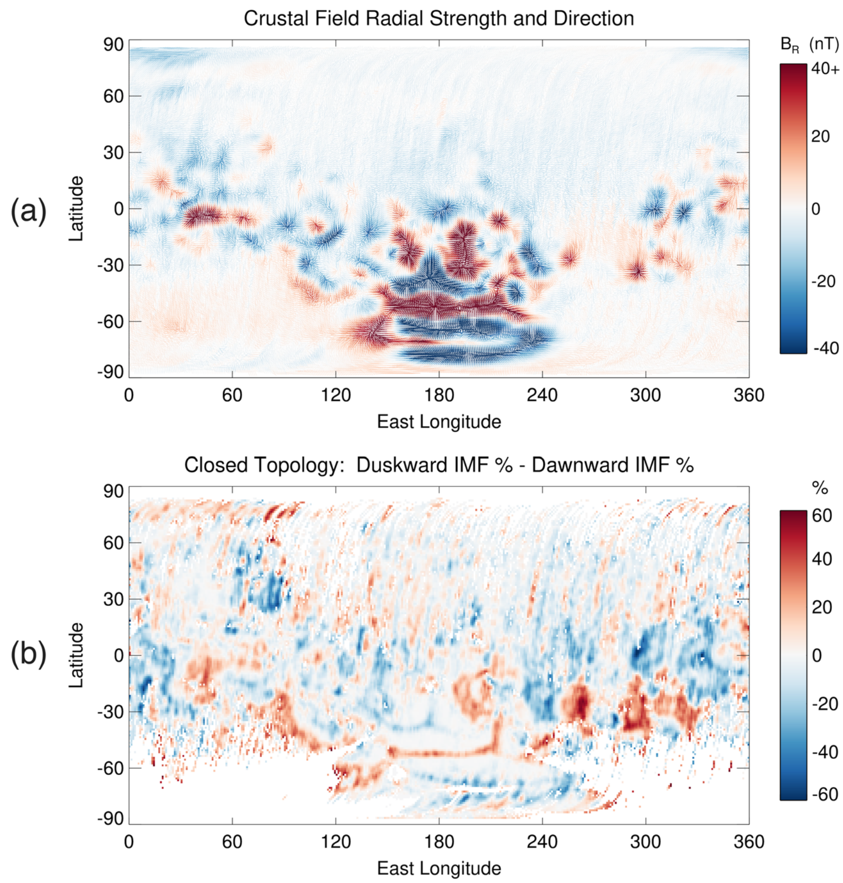

Figure 1. (a) This map of the crustal magnetic fields at 400 km altitude is adapted from Brain et al. (2003). Each 1° by 1° bin contains a vector whose length and direction correspond to the median horizontal field component measured in that bin by MGS. These vectors are colored by the median radial field component of that bin, with red signifying fields directed upward and blue signifying fields directed downward. (b) This map shows the difference in how often closed field topology was observed by MGS at 2 a.m. local time for dawnward and duskward IMF configurations. For each 1° × 1° bin, the color represents the percentage of observations that showed closed topology during duskward IMF minus the percentage that showed closed topology during dawnward IMF.

Magnetic topology at Mars is dynamic, evolving constantly as the interaction between the planet and the solar wind changes. As crustal magnetic fields rotate with the planet, they are frequently exposed to new lines of draped IMF that may be favorable for reconnection. This means that individual crustal field loops are likely to vary between open and closed topology on the timescale of Mars's rotation. Meanwhile, upstream solar wind parameters can also change substantially on an hourly timescale, affecting the entire Martian system as they do. Variations in solar wind dynamic pressure are seen to influence the overall structure of the planet's magnetosphere (Ma et al., 2002; Verigin et al., 1993) and were shown recently to drive planet-wide changes in the topology of Martian crustal fields (Weber et al., 2019). Similarly, IMF direction has been demonstrated to control the morphology and topology of the Martian magnetotail (DiBraccio et al., 2018). However, there has not yet been a direct analysis of how topology in Martian crustal field regions is influenced by upstream IMF direction. Here we present an analysis of this kind, using measurements of electron flux and magnetic field to investigate how the direction of the IMF influences whether crustal magnetic fields are open or closed to the solar wind. To accomplish this, we use data from both the Mars Global Surveyor (MGS) and Mars Atmosphere and Volatile Evolution (MAVEN) spacecraft, making use of the high data density of the former as well as the large parameter space of the latter.

In section 2 of this study we present results using MGS data, including a description of our methodology and an explanation for the trends we observe. In section 3 we evaluate these results further using MAVEN data, verifying our proposed explanation. And in section 4 we discuss the broader implications of our findings and suggest future avenues of investigation.

10.1029/2020GL087757

2. MGS Analysis

2.1. Instruments and Data Collection

The analysis of MGS data conducted here is based directly on that of Brain et al. (2007), using the same method of topology analysis as was presented in that study. This involves the identification of characteristic electron pitch angle distributions (PADs) as measured by the MGS Magnetometer and Electron Reflectometer (MAG/ER). ER was a top hat electrostatic analyzer designed to measure directional electron energy fluxes across a range of energies from 10 eV to 20 keV, and these directional fluxes are then coupled with vector magnetic field measurements from MAG to produce electron PADs (Mitchell et al., 2001). Following the method of Brain et al. (2007), we use PADs calculated from the energy channel that spans from 95 to 148 eV, as these energies provide the highest signal-to-noise for the purpose of this analysis. By analyzing these electron PADs in search of characteristic PAD shapes, we are able to determine whether or not the magnetic field lines that MGS encounters are connected to the Martian atmosphere. In particular, we take any distributions with one-sided loss cones in the return flux to represent open field lines, while two-sided loss cones and electron depletions (sometimes called “voids”) are indicative of closed fields. For a full description of the topology identification method, including an explanation of which data were excluded, refer to section 2 of Brain et al. (2007)

2.2. IMF Determination

To study the influence of IMF direction, we organize our data using an IMF proxy that was presented in Brain, Mitchell, and Halekas (2006). This proxy uses direct measurements of magnetic field direction within a region of the weakly magnetized Northern Hemisphere of Mars to infer the draping direction of the IMF. The measurements are orbit averaged, with the assumption that external conditions do not change appreciably during each 2 hr orbit. While it is unlikely that the IMF actually remained constant during each orbit, the proxy has been shown to perform well on average, and we expect that for the large-scale statistics presented here the orbit-averaged measurements should still group the data meaningfully.

For each orbit we then calculate an IMF clock angle and use this to separate our data into periods of “duskward” and “dawnward” IMF. Duskward corresponds to IMF pointing toward the dusk side of the planet (eastward on the dayside), and dawnward corresponds to clock angles pointing toward dawn (westward on the dayside), distinctions that are used throughout the rest of this paper.

2.3. Results

In Figure 1b, adapted from Brain et al. (2020), we use 7 years of MGS PAD measurements to explore how crustal magnetic field topology on the nightside of Mars changes during different IMF configurations. We begin our analysis on the nightside as this is the region most accurately studied by our method (active photoelectron production on the dayside tends to isotropize PADs and drown out any other signatures). Using characteristic PAD shapes, we create a geographic map in which each $1^\circ \times 1^\circ$ bin is colored by the difference in how often closed topology was observed during periods of duskward and dawnward IMF. Regions colored red exhibited closed topology more frequently during duskward IMF, while those colored blue showed closed topology more often during dawnward IMF.

There are several trends of note in this figure. First, as Brain et al. (2020) have pointed out, we can see that the strongest crustal field complexes show little to no variation with changes in IMF direction. Rather, the strongest changes seem to be located in regions of more moderate field strength (e.g., the crustal fields between 240° and 300° longitude and −30–0° latitude). This is a fairly intuitive result, suggesting that at MGS's fixed altitude of 400 km the centers of the large crustal field loops are effectively isolated from the influence of any externally imposed fields, while the smaller crustal fields are more susceptible to change at this altitude.

Second, the areas located between the strong crustal field arcades, typically referred to as “cusp” regions, also show a large amount of variation. Cusps have previously been shown to most frequently contain open field lines, allowing for energy transfer and ionospheric outflow, but here we see that they will also often exhibit closed topology depending on the incoming IMF configuration. In several cusp regions, closed topology observation frequencies vary with IMF direction by as much as 50 percentage points. For some cusps, closed topology occurs more often during duskward IMF, while for others closed topology is more prevalent during dawnward IMF, and a comparison with the crustal field map shown in Figure 1a reveals that this is correlated with each cusp's radial magnetic field direction. In particular, cusps that are directed radially outward show

10.1029/2020GL087757

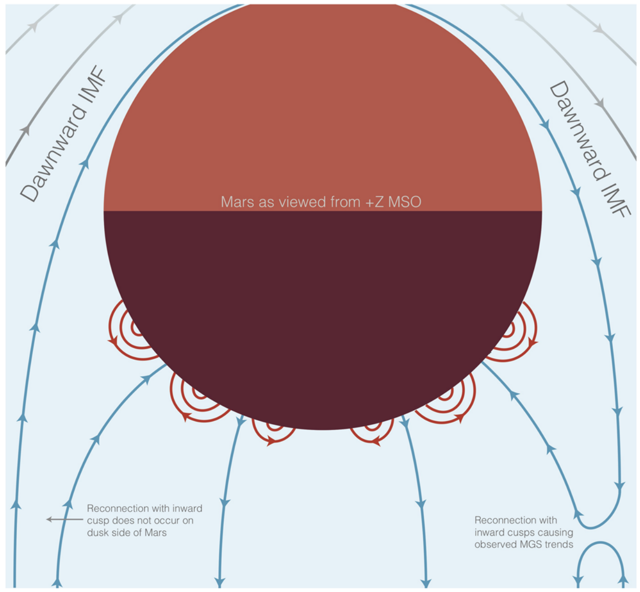

Figure 2. An illustration of open field lines from the dayside and nightside of Mars reconnecting to form a large day-to-night closed loop. Many of these dayside open field lines are in reality draped lines of IMF that thread through the ionosphere. These should follow the general draping direction of the IMF, which is represented here by the black lines. Note that the faded black lines at the bottom of the figure are intended to illustrate the draping direction and the three-dimensional nature of the situation, and do not necessarily fall into the same plane as the open field lines in the figure.

closed topology more often for duskward IMF (i.e., crustal field regions colored red in Figure 1a are also colored red in Figure 1b), while those that are directed radially inward are closed more often when the IMF is directed dawnward (i.e. crustal field regions colored blue in Figure 1a are also colored blue in Figure 1b). Note that this trend does not hold throughout the unmagnetized Northern Hemisphere, where the smaller magnitude variations should be treated as noise.

The implication here is that IMF direction determines which crustal field cusps are most likely to be closed or open to the solar wind, with a dependence on cusp radial magnetic field direction. We believe that this is due to open cusp fields reconnecting with fields in the magnetotail, a process that inherently depends on the prevailing direction of the draped IMF. We explore this in more detail below, with a simplified schematic of our explanation shown in Figure 2.

In interpreting this result, it is important to keep in mind that we are only looking at nightside results and that nightside data from MGS was all located at 2 a.m. local time. This fixed local time meant that for a given IMF direction there was a prevailing draped field direction encountered by MGS. Specifically, duskward IMF leads to draped fields near 2 a.m. primarily pointing toward the planet, while for dawnward IMF they are primarily pointing away from the planet.

With this in mind, we can then note that open cusp field lines extend into these magnetotail lobes and that those directed opposite the direction of the lobe field are in a favorable orientation to reconnect with tail field lines. This means that cusps directed radially inward may be likely to reconnect with the tail during periods of dawnward IMF, whereas those directed outward would not, remaining as unaffected open field lines. This is illustrated in Figure 2. Outward cusps should therefore have open topology more frequently (and closed topology less frequently) during dawnward IMF, as we observe in Figure 1b. But in order to understand why they often end up closed during periods of duskward IMF, it is helpful to consider the possible outcomes that result from the reconnection of an individual field line.

When an open field line from a crustal cusp reconnects with a field line in the magnetotail, the resulting topology depends on the initial topology of the tail field line. If the tail field it reconnects with was draped, then the resulting field line coming out of the cusp will still be open, meaning there has been no change in topology. If the tail field it reconnects with was another open field, however, the resulting field line will now be a closed loop. A simplified illustration of this is shown in Figure 2. Here one might note that other open fields will not necessarily be oriented in the same direction as the tail lobe, and as such might not be a likely source for frequent reconnection. However, it is important to consider that by "open" we are referring not just to field lines connecting down to crustal magnetic field sources but also to draped lines of IMF deeply embedded in the Martian ionosphere. These draped field lines connect the exobase to the solar wind, so in the context of atmospheric escape and topology identification they are treated as open fields, but importantly, they are oriented in the same direction as the tail lobes. Recent studies have shown that these open and embedded draped fields make up a sizeable portion of the magnetotail, particularly in the inner sections of the tail near the Mars-Sun line (DiBraccio et al., 2018; Xu et al., 2020).

Because these fields are common throughout the tail, it is expected that oppositely directed cusps should sometimes reconnect with them, producing loops that connect the dayside and nightside of Mars. Such a situation was observed by Xu et al. (2016), who found the presence of dayside photoelectron signatures deep on the nightside of the planet. The occurrence rate of these loops was investigated further in Xu et al. (2017), with certain regions in the Northern Hemisphere showing nightside photoelectron signatures 20–30% of the time. Here we suggest that day-night closed loops also frequently reach all the way to crustal field cusps on the nightside, throughout the strongest crustal field complexes as well as the more moderate crustal field regions. The observable end result is that cusp fields become topologically closed given the necessary IMF orientation, as shown by the trend in Figure 1.

To provide verification for this idea, we can search for other features that our interpretation suggests should be present. First, if these closed fields originating in cusp regions are indeed connected to the dayside of Mars, we should expect to see photoelectron signatures propagating tailward along the field line, as observed in Xu et al. (2016). Second, if the variations in cusp topology are in fact due to reconnection with field lines in the magnetotail, we should expect to observe opposite trends in the two magnetotail lobes. That is, if we believe that MGS is observing upward cusp fields at 2 a.m. reconnecting with the tail field and becoming closed, we should expect that at 10 PM local time we would instead see downward cusp fields reconnecting, as the direction of the tail field is reversed here. While the mapping orbital configuration of MGS, which was fixed at 400 km altitude and 2 a.m./2 p.m. local time, prevents us from using it to investigate this possibility, the orbit of the MAVEN spacecraft is not subject to the same constraints. In the next section, we use measurements from the MAVEN spacecraft to explore these predictions and are able to identify both of the features described here.

3. MAVEN Analysis

3.1. Identifying Topology With MAVEN

To identify magnetic topology with MAVEN, we use a technique presented in Xu et al. (2019). This method combines two different strategies for topology analysis at Mars, effectively capturing the strengths of each. One approach is that of identifying characteristic PAD shapes to determine whether electron fluxes have interacted with the Martian atmosphere. This is the same approach that was used for the MGS data analysis in this study and has also been used to map magnetic topology at Mars using MAVEN data (Weber et al., 2017). This method is very effective on the nightside of the planet but is less robust on the dayside of Mars, where the active isotropic production of photoelectrons tends to drown out the PAD shape signal. Fortunately, the dayside of the planet is the region that is most accurately studied by the second method, which uses characteristic electron energy spectra to identify whether MAVEN is encountering photoelectrons, solar wind electrons, or both. By studying the directional fluxes of these different populations, we are able to accurately determine magnetic topology across the dayside of Mars, as demonstrated in Xu et al. (2017). The combined method therefore employs these two strategies in parallel, using both sets of information to determine magnetic topology throughout the entire Martian system. A more complete description of this system of topology identification can be found in section 2.3 of Xu et al. (2019)

3.2. Instruments and Data Collection

The electron energy spectra and PADs used in this section of the study were measured using the Solar Wind Electron Analyzer (SWEA) and Magnetomenter (MAG) instruments aboard MAVEN (Connerney et al., 2015; Jakosky et al., 2015; Mitchell et al., 2016). SWEA is a hemispheric electrostatic analyzer designed to measure electron fluxes for energies ranging from 3 eV to 4.6 keV, such that it captures both ionospheric photoelectrons and solar wind electrons. These fluxes are paired with magnetic field data supplied by MAG

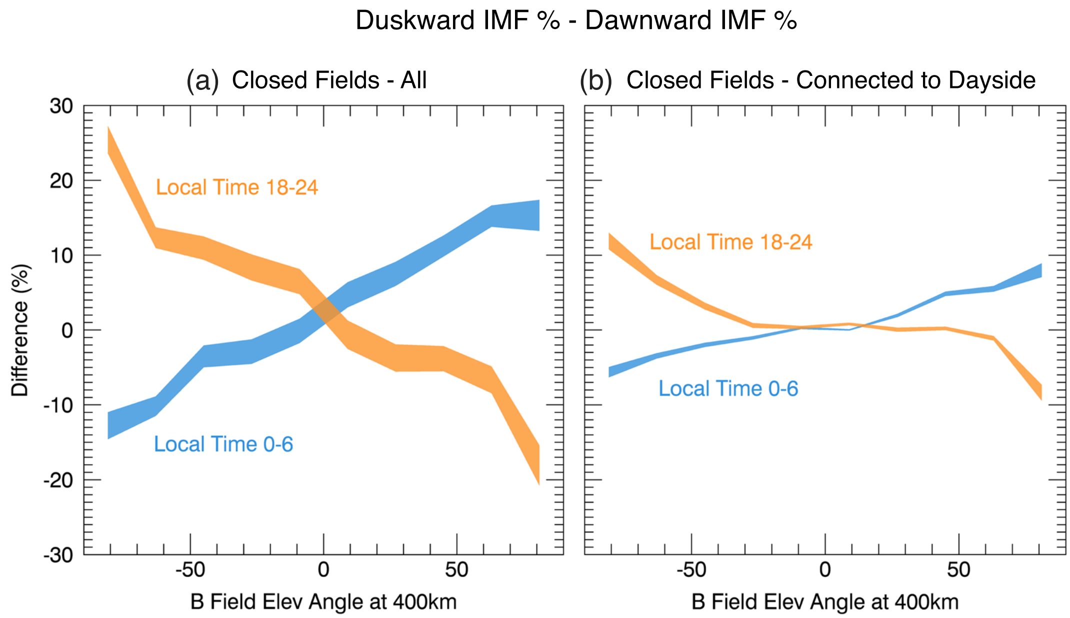

Figure 3. (a) The difference in how often closed topology was observed during periods of duskward and dawnward IMF (the same quantity as in Figure 1b), plotted as a function of crustal field elevation angle. Specifically, we are plotting the number of observations of closed topology for a specified IMF direction divided by the total number of observations made for that IMF direction. (b) The same quantity, but only considering closed fields that are connected to the dayside of Mars, as determined by the presence of photoelectron signatures.

to produce PADs and directional energy distributions, and SWEA's 360° by 120° field of view generally samples the complete range of pitch angles. Three-dimensional magnetic field measurements are provided at 32 Hz by MAG, which uses two triaxal fluxgate sensors.

Four years of MAVEN data are used in this study, from 1 December 2014 through 1 January 2019. During this time, MAVEN's precessing elliptical orbit allowed for data coverage across a wide range of local times, altitudes, crustal field strengths, and solar wind conditions. As this study is focused on the behavior of magnetic fields within the Martian ionosphere, we only use data measured below 500 km altitude. We also impose a lower limit of 200 km altitude to ensure that we generally stay above the electron exobase, where our method of identifying topology breaks down. Additionally, we only use data for which the electron PAD had some data coverage within 30° parallel and antiparallel to the field, as these field-aligned fluxes are a primary component of our method of topology identification.

3.3. IMF Measurements

As with the MGS results, we separate our MAVEN data into periods of duskward and dawnward IMF. We sort the data based on orbit-averaged measurements of the IMF, using data sampled by MAG for all times when MAVEN was located outside of the sheath. Orbits during which MAVEN did not directly sample the solar wind are excluded from this study. From these orbit-averaged measurements, we calculate IMF clock angles, where a clock angle of 0° corresponds to the $+Z$ direction and 90° corresponds to the $+Y$ direction in the MSO frame. We classify the IMF direction as duskward when the clock angle falls between 10° and 170° and dawnward when the clock angle falls between 190° and 350°.

3.4. Results

With this set of analysis tools from MAVEN, we can investigate our explanation for the results we observed with MGS. To explore our prediction that there should be reversed trends on opposite sides of the current sheet, we present Figure 3a, which studies cusp response to IMF direction as a function of local time. Because we are specifically investigating crustal field variations here, we prune our data to only include measurements where the modeled crustal field strength was greater than 15 nT at MAVEN's location. In order to make a direct comparison to our MGS results, we plot the same quantity here as in Figure 1b. However, MAVEN's data coverage is not yet sufficient at all geographic locations for us to produce a comparable map, so we instead plot this as a function of crustal field elevation angle. The behavior of cusps directed outward can therefore be found on the right half of the plot and that of cusps directed inward on the left half of the plot.

The results are then divided into two local time segments, corresponding to rough boundaries for the two lobes of the magnetosphere. The blue line (local time 0–6) represents the same region of space as was sampled by MGS, and it shows the same trend. Outward cusps are closed more often during periods of duskward IMF, while inward cusps are closed more often during periods of dawnward IMF. For the orange line (local time 18–24), which represents the opposite side of the current sheet from MGS, this trend is reversed. Outward cusps are closed more often during periods of dawnward IMF, and inward cusps are closed more often during periods of duskward IMF. This dependence on magnetotail direction is consistent with our hypothesis that the cusp phenomenon observed involves reconnection with tail fields.

We next investigate our suggestion that these reconnecting fields should frequently end up connected to the dayside of the planet. To verify this, we make use of the fact that our method for identifying topology uses photoelectron energy signatures to determine whether a field line is connected to the dayside ionosphere. This allows us to distinguish between closed field lines on the dayside and nightside, and here allows us to determine whether these cusp fields are connected to the dayside of Mars. In Figure 3b, we use the same format and same set of data as in Figure 3a, but this time only labeling fields as "closed" if they connect to the dayside of Mars and are determined to be closed using electron energy and PAD signatures, as detailed in Xu et al. (2019). The trend we are investigating remains clearly visible, with the variations being slightly reduced in size. This suggests that a sizeable fraction of the variations we observe are due to field lines reconnecting to the dayside of the planet. For example, we see in Figure 3a that during duskward IMF, cusps directed vertically inward at local time 18–24 are closed 20 percentage points more often than during dawnward IMF. By comparison to panel (b) we can see that half of this variation (10 percentage points) is due to connections to the dayside of Mars. The remaining half of the variation is therefore due to closed loops forming that are connected solely to the nightside.

4. Discussion and Conclusion

The results shown in this paper hold several implications worth noting. First, incoming IMF direction directly influences, which crustal field cusps are open or closed to the solar wind. While we would expect that the IMF should interact with crustal fields regularly, the fact that cusps on the nightside are also greatly influenced by IMF direction is a reminder that the entire Martian system is extremely susceptible to changes in upstream conditions and that these crustal magnetic sources are malleable at all locations around the planet. The relationship we demonstrate between IMF direction and cusp topology could also help inform modeling efforts at Mars, particularly any that are interested in mapping plasma flows all the way down to the planet's ionosphere.

Second, because cusp topology appears to depend on magnetotail field direction, it is likely that many cusps transition between closed and open as they rotate through the nightside and encounter both tail lobes. This suggests that cusp regions are dynamic on a daily or hourly timescale, potentially experiencing a convective cycle of sorts. The current sheet in particular would be a region where many topological changes might occur, as it represents the transition between the tail lobes. This could potentially lead to energetic processes and enhanced particle outflow in this area.

Third, crustal field cusps on the nightside are frequently connected to the dayside via large-scale closed loops. This adds another dimension to the results found in the weakly magnetized Northern Hemisphere by Xu et al. (2016). As discussed in that paper, magnetic connections to the dayside ionosphere act as source of localized energy input in the form of precipitating electrons. This should lead to increases in particle ionization rates and temperatures and could be a source for the low-energy discrete aurora observed by Mars Express (Leblanc et al., 2006), all of which could potentially drive ion outflow. Cusp regions in particular, more than weakly magnetized regions, should channel energy input from the dayside into small areas, while also containing the vertically oriented magnetic fields that are particularly conducive to particle escape (e.g., Ergun et al., 2016). It is also important to note here that although these field lines are topologically closed in the context of electron transfer, most ions are not expected to be constrained in the same way. Those that travel into these large closed loops, either from the dayside or the nightside, will likely have gyroradii on the order of tens of kilometers, and could easily drift onto other field lines that may or may not lead back into the Martian ionosphere.

Finally, in this paper we only considered crustal fields on the nightside of Mars, but we expect that those on the dayside should also respond significantly to IMF variations. This response should be very different, however, as the dayside interaction with the IMF is a situation unlike that on the nightside. Draped lines of IMF are pressed down to low altitudes, interacting directly with the loop tops of closed crustal fields. Reconnection between draped fields and these loop tops is expected to occur frequently and could lead to variations in crustal field size and location. We also note that throughout much of the strong crustal field anomaly, these loop tops have a north-south orientation. This means that it may be the north/south component of the IMF (rather than the duskward/dawnward component) that has the largest influence on dayside crustal field topology, a prediction that could be examined through future data analysis and modeling studies.

Data Availability Statement

All MAVEN data used in this work are available through the Planetary Data System (https://pds-ppi.igpp.ucla.edu/mission/MAVEN).

Acknowledgments
The authors thank Laila Andersson, James McFadden, and Yaxue Dong for their calculations of spacecraft potential, which in this study are used to correct electron energy distributions. Parts of this work for the observations obtained with the SWEA instrument are supported by the French space agency CNES.

References

Acuna, M. H., Connerney, J. E. P., Wasilewski, P., Lin, R. P., Anderson, K. A., Carlson, C. W., et al. (1998). Magnetic field and plasma observations at Mars: Initial results of the Mars Global Surveyor Mission. *Science*, *279*(5357), 1676–1680.

Brain, D. A., Bagenal, F., Acuña, M. H., & Connerney, J. E. P. (2003). Martian magnetic morphology: Contributions from the solar wind and crust. *Journal of Geophysical Research*, *108*(A12), 1424. https://doi.org/10.1029/2002JA009482

Brain, D. A., Baker, A. H., Briggs, J., Eastwood, J. P., Halekas, J. S., & Phan, T.-D. (2010). Episodic detachment of Martian crustal magnetic fields leading to bulk atmospheric plasma escape. *Geophysical Research Letters*, *37*, L14108. https://doi.org/10.1029/2010GL043916

Brain, D. A., Halekas, J. S., Peticolas, L. M., Lin, R. P., Luhmann, J. G., Mitchell, D. L., et al. (2006). On the origin of aurorae on Mars. *Geophysical Research Letters*, *33*, L01201. https://doi.org/10.1029/2005GL024782

Brain, D. A., Lillis, R. J., Mitchell, D. L., Halekas, J. S., & Lin, R. P. (2007). Electron pitch angle distributions as indicators of magnetic field topology near Mars. *Journal of Geophysical Research*, *112*, A09201. https://doi.org/10.1029/2007JA012435

Brain, D. A., Mitchell, D. L., & Halekas, J. S. (2006). The magnetic field draping direction at Mars from April 1999 through august 2004. *Icarus*, *182*(2), 464–473.

Brain, D. A., Weber, T., Xu, S., Mitchell, D., Lillis, R., Halekas, J., et al. (2020). Variations in night side magnetic field topology at Mars. *Geophysical Research Letters*, *47*, e2020GL088921. https://doi.org/10.1029/2020GL088921

Collinson, G., Mitchell, D., Glocer, A., Grebowsky, J., Peterson, W. K., Connerney, J., et al. (2015). Electric Mars: The first direct measurement of an upper limit for the Martian polar wind electric potential. *Geophysical Research Letters*, *42*, 9128–9134. https://doi.org/10.1002/2015GL065084

Connerney, J. E. P., Espley, J., Lawton, P., Murphy, S., Odom, J., Oliversen, R., & Sheppard, D. (2015). The maven magnetic field investigation. *Space Science Reviews*, *195*(1–4), 257–291.

DiBraccio, G. A., Luhmann, J. G., Curry, S. M., Espley, J. R., Xu, S., Mitchell, D. L., et al. (2018). The twisted configuration of the Martian magnetotail: MAVEN observations. *Geophysical Research Letters*, *45*, 4559–4568. https://doi.org/10.1029/2018GL077251

Dubinin, E. M., Fraenz, M., Woch, J., Roussos, E., Winningham, J. D., Frahm, R. A., et al. (2008). Access of solar wind electrons into the Martian magnetosphere. *Annales Geophysicae*, *26*, 3511–3524.

Dubinin, E. M., Fraenz, M., Woch, J., Winnigham, J. D., Frahm, R., Lundin, R., & Barabash, S. (2008). Suprathermal electron fluxes on the nightside of Mars: ASPERA-3 observations. *Planetary and Space Science*, *56*(6), 846–851.

Eastwood, J. P., Brain, D. A., Halekas, J. S., Drake, J. F., Phan, T. D., Øieroset, M., et al. (2008). Evidence for collisionless magnetic reconnection at Mars. *Geophysical Research Letters*, *35*, L02106. https://doi.org/10.1029/2007GL032289

Ergun, R. E., Andersson, L. A., Fowler, C. M., Woodson, A. K., Weber, T. D., Delory, G. T., et al. (2016). Enhanced O2+ loss at Mars due to an ambipolar electric field from electron heating. *Journal of Geophysical Research: Space Physics*, *121*, 4668–4678. https://doi.org/10.1002/2016JA022349

Fillingim, M. O., Peticolas, L. M., Lillis, R. J., Brain, D. A., Halekas, J. S., Lummerzheim, D., & Bougher, S. W. (2010). Localized ionization patches in the nighttime ionosphere of Mars and their electrodynamic consequences. *Icarus*, *206*(1), 112–119.

Fillingim, M. O., Peticolas, L. M., Lillis, R. J., Brain, D. A., Halekas, J. S., Mitchell, D. L., et al. (2007). Model calculations of electron precipitation induced ionization patches on the nightside of Mars. *Geophysical Research Letters*, *34*, L12101. https://doi.org/10.1029/2007GL029986

Fox, J. L., Brannon, J. F., & Porter, H. S. (1993). Upper limits to the nightside ionosphere of Mars. *Geophysical Research Letters*, *20*(13), 1339–1342.

Fox, J. L., & Dalgarno, A. (1979). Ionization, luminosity, and heating of the upper atmosphere of Mars. *Journal of Geophysical Research*, *84*(A12), 7315–7333.

Frahm, R. A., Sharber, J. R., Winningham, J. D., Wurz, P., Liemohn, M. W., Kallio, E., et al. (2006). Locations of atmospheric photoelectron energy peaks within the Mars environment. *Space Science Reviews*, *126*(1–4), 389–402.

Haider, S. A., Kim, J., Nagy, A. F., Keller, C. N., Verigin, M. I., Gringauz, K. I., et al. (1992). Calculated ionization rates, ion densities, and airglow emission rates due to precipitating electrons in the nightside ionosphere of Mars. *Journal of Geophysical Research*, *97*(A7), 10,637–10,641.

Harnett, E. M., & Winglee, R. M. (2006). Three-dimensional multifluid simulations of ionospheric loss at Mars from nominal solar wind conditions to magnetic cloud events. *Journal of Geophysical Research*, *111*, A09213. https://doi.org/10.1029/2006JA011724

Jakosky, B. M., Brain, D., Chaffin, M., Curry, S., Deighan, J., Grebowsky, J., et al. (2018). Loss of the Martian atmosphere to space: Present-day loss rates determined from maven observations and integrated loss through time. *Icarus*, *315*, 146–157.

Jakosky, B. M., Lin, R. P., Grebowsky, J. M., Luhmann, J. G., Mitchell, D. F., Beutelschies, G., et al. (2015). The Mars Atmosphere and Volatile Evolution (MAVEN) mission. *Space Science Reviews*, *195*(1–4), 3–48.

Krymskii, A. M., Ness, N. F., Crider, D. H., Breus, T. K., Acuna, M. H., & Hinson, D. P. (2004). Solar wind interaction with the ionosphere/atmosphere and crustal magnetic fields at Mars: Mars Global Surveyor magnetometer/electron reflectometer, radio science, and accelerometer data. *Journal of Geophysical Research*, *109*, A11306. https://doi.org/10.1029/2004JA010420

Leblanc, F., Witasse, O., Lilensten, J., Frahm, R. A., Safaenili, A., Brain, D. A., et al. (2008). Observations of aurorae by SPICAM ultraviolet spectrograph on board Mars Express: Simultaneous ASPERA-3 and MARSIS measurements. *Journal of Geophysical Research*, *113*, A08311. https://doi.org/10.1029/2008JA013033

Leblanc, F., Witasse, O., Winningham, J., Brain, D., Lilensten, J., Blelly, P.-L., et al. (2006). Origins of the Martian aurora observed by Spectroscopy for Investigation of Characteristics of the Atmosphere of Mars (SPICAM) on board Mars Express. *Journal of Geophysical Research*, *111*, A09313. https://doi.org/10.1029/2006JA011763

Liemohn, M. W., Ma, Y., Frahm, R. A., Fang, X., Kozyra, J. U., Nagy, A. F., et al. (2007). Mars global MHD predictions of magnetic connectivity between the dayside ionosphere and the magnetospheric flanks. In C. T. Russell (Ed.), *The Mars plasma environment* (pp. 63–76). New York, NY: Springer.

Liemohn, M. W., Ma, Y., Nagy, A. F., Kozyra, J. U., Winningham, J. D., Frahm, R. A., et al. (2007). Numerical modeling of the magnetic topology near Mars auroral observations. *Geophysical Research Letters*, *34*, L24202. https://doi.org/10.1029/2007GL031806

Lillis, R. J., & Brain, D. A. (2013). Nightside electron precipitation at Mars: Geographic variability and dependence on solar wind conditions. *Journal of Geophysical Research: Space Physics*, *118*, 3546–3556. https://doi.org/10.1002/jgra.50171

Lillis, R. J., & Fang, X. (2015). Electron impact ionization in the Martian atmosphere: Interplay between scattering and crustal magnetic field effects. *Journal of Geophysical Research: Planets*, *120*, 1332–1345. https://doi.org/10.1002/2015JE004841

Lillis, R. J., Fillingim, M. O., & Brain, D. A. (2011). Three-dimensional structure of the Martian nightside ionosphere: Predicted rates of impact ionization from Mars global surveyor magnetometer and electron reflectometer measurements of precipitating electrons. *Journal of Geophysical Research*, *116*, A12317. https://doi.org/10.1029/2011JA016982

Lillis, R. J., Fillingim, M. O., Peticolas, L. M., Brain, D. A., Lin, R. P., & Bougher, S. W. (2009). Nightside ionosphere of Mars: Modeling the effects of crustal magnetic fields and electron pitch angle distributions on electron impact ionization. *Journal of Geophysical Research*, *114*, E11009. https://doi.org/10.1029/2009JE003379

Lillis, R. J., Mitchell, D. L., Steckiewicz, M., Brain, D., Xu, S., Weber, T., et al. (2018). Ionizing electrons on the Martian nightside: Structure and variability. *Journal of Geophysical Research: Space Physics*, *123*, 4349–4363. https://doi.org/10.1029/2017JA025151

Luhmann, J. G., Dong, C., Ma, Y., Curry, S. M., Mitchell, D., Espley, J., et al. (2015). Implications of MAVEN Mars near-wake measurements and models. *Geophysical Research Letters*, *42*, 9087–9094. https://doi.org/10.1002/2015GL066122

Ma, Y., Fang, X., Russell, C. T., Nagy, A. F., Toth, G., Luhmann, J. G., et al. (2014). Effects of crustal field rotation on the solar wind plasma interaction with Mars. *Geophysical Research Letters*, *41*, 6563–6569. https://doi.org/10.1002/2014GL060785

Ma, Y., Nagy, A. F., Hansen, K. C., DeZeeuw, D. L., Gombosi, T. I., & Powell, K. G. (2002). Three-dimensional multispecies mhd studies of the solar wind interaction with Mars in the presence of crustal fields. *Journal of Geophysical Research*, *107*(A10), 1282. https://doi.org/10.1029/2002JA009293

Mitchell, D. L., Lin, R. P., Mazelle, C., Rème, H., Cloutier, P. A., Connerney, J. E. P., et al. (2001). Probing Mars' crustal magnetic field and ionosphere with the MGS electron reflectometer. *Journal of Geophysical Research*, *106*(E10), 23,419–23,427.

Mitchell, D. L., Mazelle, C., Sauvaud, J.-A., Thocaven, J.-J., Rouzaud, J., Fedorov, A., et al. (2016). The MAVEN solar wind electron analyzer. *Space Science Reviews*, *200*(1–4), 495–528.

Němec, F., Morgan, D. D., Gurnett, D. A., & Brain, D. A. (2011). Areas of enhanced ionization in the deep nightside ionosphere of Mars. *Journal of Geophysical Research*, *116*, E06006. https://doi.org/10.1029/2011JE003804

Nilsson, H., Edberg, N. iklasJ. T., Stenberg, G., Barabash, S., Holmström, M., Futaana, Y., et al. (2011). Heavy ion escape from Mars, influence from solar wind conditions and crustal magnetic fields. *Icarus*, *215*(2), 475–484.

Ramstad, R., Barabash, S., Futaana, Y., Nilsson, H., & Holmström, M. (2016). Effects of the crustal magnetic fields on the Martian atmospheric ion escape rate. *Geophysical Research Letters*, *43*, 10,574–10,579. https://doi.org/10.1002/2016GL070135

Sakai, S., Andersson, L., Cravens, T. E., Mitchell, D. L., Mazelle, C., Rahmati, A., et al. (2016). Electron energetics in the Martian dayside ionosphere: Model comparisons with MAVEN data. *Journal of Geophysical Research: Space Physics*, *121*, 7049–7066. https://doi.org/10.1002/2016JA022782

Verigin, M. I., Gringauz, K. I., Kotova, G. A., Remizov, A. P., Shutte, N. M., Rosenbauer, H., et al. (1993). The dependence of the Martian magnetopause and bow shock on solar wind RAM pressure according to Phobos 2 TAUS ion spectrometer measurements. *Journal of Geophysical Research*, *98*(A2), 1303–1309.

Weber, T., Brain, D., Mitchell, D., Xu, S., Connerney, J., & Halekas, J. (2017). Characterization of low-altitude nightside Martian magnetic topology using electron pitch angle distributions. *Journal of Geophysical Research: Space Physics*, *122*, 9777–9789. https://doi.org/10.1002/2017JA024491

Weber, T., Brain, D., Mitchell, D., Xu, S., Espley, J., Halekas, J., et al. (2019). The influence of solar wind pressure on Martian crustal magnetic field topology. *Geophysical Research Letters*, *46*, 2347–2354. https://doi.org/10.1029/2019GL081913

Xu, S., Liemohn, M. W., & Mitchell, D. L. (2014). Solar wind electron precipitation into the dayside Martian upper atmosphere through the cusps of strong crustal fields. *Journal of Geophysical Research: Space Physics*, *119*, 10,100–10,115. https://doi.org/10.1002/2014JA020363

Xu, S., Mitchell, D., Liemohn, M., Dong, C., Bougher, S., Fillingim, M., et al. (2016). Deep nightside photoelectron observations by MAVEN SWEA: Implications for Martian Northern Hemispheric magnetic topology and nightside ionosphere source. *Geophysical Research Letters*, *43*, 8876–8884. https://doi.org/10.1002/2016GL070527

Xu, S., Mitchell, D., Liemohn, M., Fang, X., Ma, Y., Luhmann, J., et al. (2017). Martian low-altitude magnetic topology deduced from MAVEN/SWEA observations. *Journal of Geophysical Research: Space Physics*, *122*, 1831–1852. https://doi.org/10.1002/2016JA023467

Xu, S., Mitchell, D. L., Weber, T., Brain, D. A., Luhmann, J. G., Dong, C., et al. (2020). Characterizing Mars magnetotail topology with respect to the upstream interplanetary magnetic fields. *Journal of Geophysical Research: Space Physics*, *125*, e2019JA027755. https://doi.org/10.1029/2019JA027755

Xu, S., Weber, T., Mitchell, D. L., Brain, D. A., Mazelle, C., DiBraccio, G. A., & Espley, J. (2019). A technique to infer magnetic topology at Mars and its application to the terminator region. *Journal of Geophysical Research: Space Physics*, *124*, 1823–1842. https://doi.org/10.1029/2018JA026366